An automated survey design process to reduce the environmental impact of onshore seismic surveys

Tim Dean[1], Jennifer Whitfield[1], Julia Miller[2], and Peter Brady[3]

https://doi.org/10.1190/tle41110786.1

Check for updates

Downloaded 11/14/22 to 76.133.148.255. Redistribution subject to SEG license or copyright; see Terms of Use at http://library.seg.org/page/policies/terms
DOI:10.1190/tle41110786.1

Abstract

Land seismic surveys acquired in anything but the barest landscapes encounter obstacles that cause the planned survey points to be either shifted or skipped. Besides these forced changes, an increased awareness of the environmental impact of seismic surveys, coupled with a general lack of trust and even opposition to the traditional energy industry, has resulted in a demand to minimize the impacts of the clearing that is necessary to allow access to the survey lines. We present a method to reduce the environmental impact of seismic surveys without compromising seismic imaging. The process is straightforward and can be applied automatically using standard mathematical software (in this case, MATLAB). For the example shown here, where the line spacing was particularly dense, the impact on vegetation greater than 2 m in height was reduced by 55%. For less dense geometries, where there is more opportunity to offset points, the impact is likely to be larger.

Introduction

Land seismic surveys acquired in anything but the barest landscapes encounter obstacles that cause the source and/or receiver points to be shifted from their ideal positions or even skipped. Besides forced changes to survey lines, such as those imposed by rugged terrain, we may also wish to minimize the environmental impacts of the clearing necessary for survey lines by detouring around vegetation rather than creating dead-straight survey lines (e.g., Figure 1). Thus, the impacts to flora, vegetation, fauna habitat, fauna breeding places, or individual fauna that arise from clearing can be minimized or avoided.

The removal of greater quantities and/or more established vegetation increases the time it takes for the environment to recover. Slow vegetation recovery can lead to lasting landscape fragmentation and impacts to biodiversity and ecosystem processes (Dabros et al., 2018), such as introducing dieback and promoting the establishment and propagation of weeds.

Cleared lines enable predators to move more easily, reducing the areas of suitable habitat for prey animals that are forced to avoid them (Latham et al., 2011) or increasing the chances of encounters when both animals preferentially use the cleared areas for movement (Dawson et al., 2018). In particular, straight lines enhance the line of sight for potential predators (Embar et al., 2011).

It is therefore desirable to develop a strategy that enables survey-line-placement planning to consider biodiversity concerns such as the establishment of a buffer around animal breeding sites, nesting places, flora, vegetation communities, or fauna habitat identified from ecological surveys. Enabling survey line placement to inherently prevent or minimize the introduction and spread of weed species or vegetation dieback is also desirable.

To minimize the effects on the survey, a number of different strategies have been developed over the years. Originally, these relied on simply offsetting points (moves in the crossline direction, Figure 2b) and/or skidding points (moves in the inline direction, Figure 2c). Donze and Crews (2000) define a strategy based on the following hierarchy:

1) Skidding the point: recommended maximum skids are either a quarter of the point interval (Donze and Crews, 2000) or half the point interval (Cordsen et al., 2000), the latter representing the maximum that can be applied without the common-depth point falling in a different bin (Figure 2c).
2) Offsetting points: keeping offsets to less than half the point interval preserves fold (Figure 2b). The maximum offset distance recommended by Donze and Crews (2000) is half the shot line spacing.
3) Skid the point by a distance equal to the receiver line spacing, and acquire an additional line of receivers.
4) Skid the point by a distance equal to the receiver line spacing and offset the point (i.e., a combination of 2 and 3). Note that you cannot offset and skid by a full bin width and have no effect on fold. Instead, the total distance from the planned point must be less than one full bin width. It should be noted that the efficiency of skidding versus offsetting depends on the shape of the exclusion zone. For a circular exclusion zone, skidding is less effective than offsetting. (Note that the exclusion zone on Figure 2b is farther to the north than in Figure 2c.)

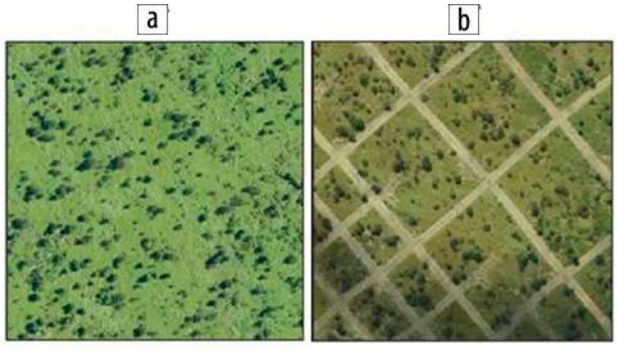

Figure 1. Aerial photos taken (a) before and (b) after line clearance. The denser line spacing is 24 m, and the wider spacing is 48 m. Note that the lines are dead straight.

[1]BHP, Brisbane, Australia. E-mail: tim.dean.geo@gmail.com; jennifer.whitfield@bhp.com.
[2]Aurecon, Brisbane, Australia. E-mail: julia.miller@my.jcu.edu.au.
[3]The Mathworks, Sydney, Australia. E-mail: pbrady@mathworks.com.

Downloaded 11/14/22 to 76.133.148.255. Redistribution subject to SEG license or copyright; see Terms of Use at http://library.seg.org/page/policies/terms
DOI:10.1190/tle41110786.1

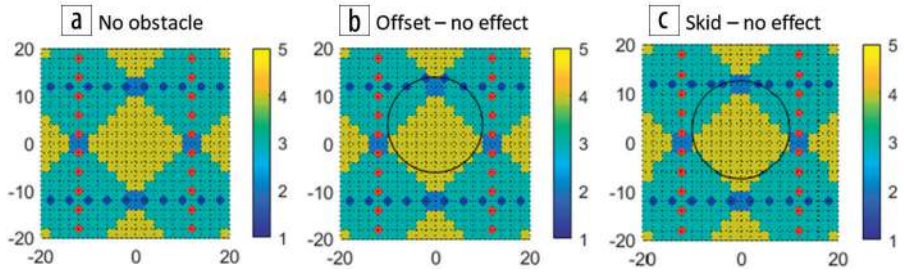

Figure 2. Fold diagrams for a simple orthogonal geometry. Two meter spaced bin edges are shown by the black dashed lines. (a) No obstacle, (b) offset by a single bin dimension (Y = 2 m), (c) skid by the maximum distance (X = 2.7 m). Note that the circular exclusion zone in (b) is further north than that in (c); i.e., offsetting is more effective than skidding in this case.

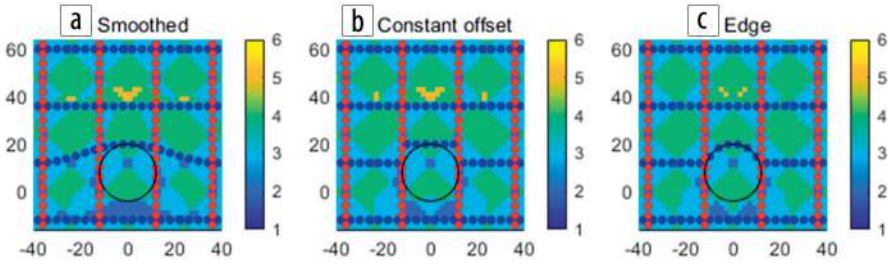

Figure 3. Fold plots, again with 4 m source and receiver spacing, showing the impact of different strategies used to offset the receiver points around a circular exclusion zone with a radius of 12 m placed at the point (0, 8).

Figure 4. Aerial photograph of a section of the survey area. The dark green areas are tree canopies, and the light green is open grassland.

Alternately, Cordsen et al. (2000) show an example offset/skid chart showing the priority of alternate point locations.

More recently, attention has turned to using automatic algorithms to adapt survey designs to account for obstacles. Bastidas and Liu (2019) develop a method for automatically applying offsets by employing a set of rules consistent with the approach of Donze and Crews (2000). Stork (2019) presents a more sophisticated survey design approach that combines a map of source and receiver costs (the cost of occupying a point within a nonpermitted area is very high) along with source and receiver noise. A random set of source and receiver locations is then created, which can be constrained to lines if required. The initial set of positions is considerably larger (approximately 20 times) than the desired number. The survey fold is then calculated using all of the points and their relative contribution to each bin along with the cost of occupying them. Through a process of point removal and small point shifting, the expanded set of survey points is then reduced to the required size.

Throughout his authoritative book on survey planning, Vermeer (2012) emphasizes the importance of spatial continuity, which he defines as the absence of spatial irregularities generated by missing points and edges. His recommended detour approach, therefore, is to have a smooth path around the point (e.g., Figure 3a) rather than skidding or offsetting points.

Of course, many of the obstacles we wish to avoid do not occupy a simple circular area such as those shown in Figures 2 and 3. Areas of vegetation, in particular, typically occupy randomly shaped, though roughly continuous, areas (e.g., Figure 4). Our objective, therefore, was to take an ideal grid of orthogonal source and receiver points and move them to minimize environmental disturbance while staying close to the original survey design and maintaining spatial continuity. The process needed to be automatic, as manually moving points would be prohibitively time consuming.

Vegetation detection

In the case presented here, the obstacles we aimed to avoid were principally vegetation, so the first stage in the process was to identify vegetated areas. This was done using LiDAR data that had been specially processed to identify vegetation heights from the secondary returns. The objective of the advanced processing was to classify the vegetation height as low (0–0.3 m), medium (0.3–2 m), or high (greater than 2 m), although other height ranges can be employed during the processing. Figure 5 shows the image included as Figure 4 with the vegetation heights superimposed. Although a few areas of vegetation have been missed (the LiDAR points have a spacing of approximately 1 m), the results are adequate for our purposes.

Downloaded 11/14/22 to 76.133.148.255. Redistribution subject to SEG license or copyright; see Terms of Use at http://library.seg.org/page/policies/terms
DOI:10.1190/tle41110786.1

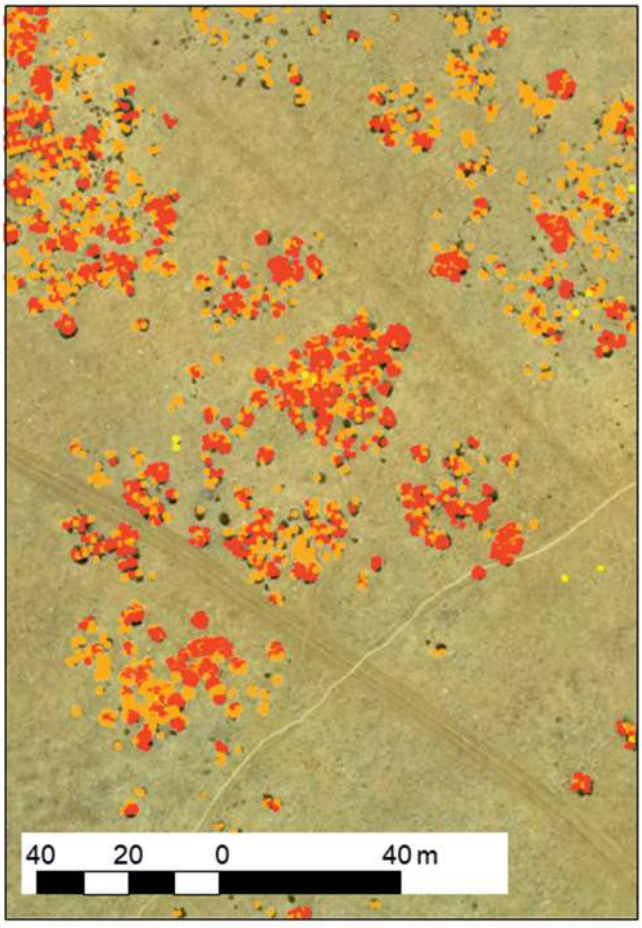

Figure 5. The aerial photograph shown in Figure 4 with the addition of the LiDAR-based vegetation classification results. The yellow points are low vegetation (0–0.3 m), the orange are medium (0.3–2 m), and the red are high (higher than 2 m).

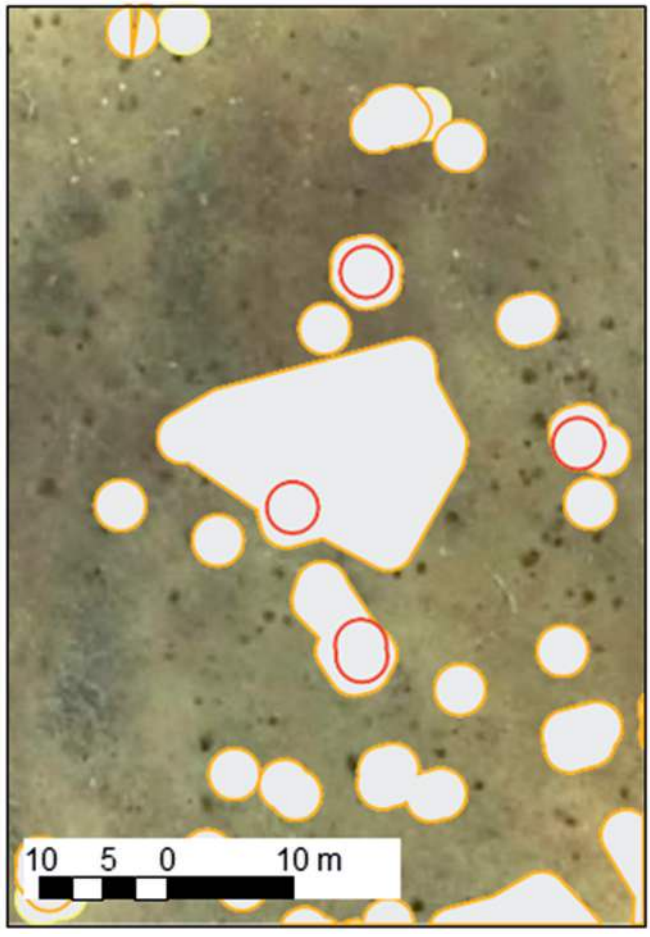

Figure 6. Vegetation height data after a buffer has been applied and the overlapping areas merged.

Once the areas of vegetation have been identified, we need to add a buffer around them to allow for the LiDAR point spacing and the width of the cleared path. Once these buffers have been applied, we then need to merge overlapping areas. Although described here as if they are two separate steps, we have found that it is more computationally efficient to merge these two stages together by applying a clustering algorithm with a suitably sized buffer. An example of the resulting areal classification is shown in Figure 6. Note that there are high and medium vegetation height areas that overlap.

Survey processing

Processing of the survey positions (in this case generated on an orthogonal grid) begins by reading the theoretical positions along each line. If the lines are not already oriented east-west, then it is computationally simpler to rotate them prior to this orientation before applying any offsets. We then create a dense grid of possible locations with a density higher than the actual point spacing. In the example shown in Figure 7, the crossline spacing is denser than the inline spacing as we only allow limited crossline offsets. (In this case, you can only offset by half the line interval.) Also note that the positions at the ends of the line are limited in the crossline direction. The crossline point spacing of the grid is 1 m. If the effect of the detours needs to be minimized further, this spacing can be reduced.

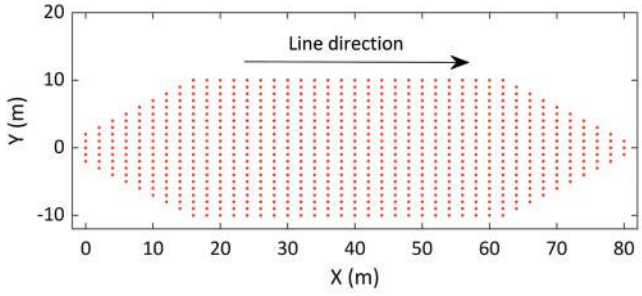

Figure 7. Grid of possible positions generated for an east-west line. Note that the crossline point spacing is denser than the inline spacing as we are only allowing crossline offsets.

Another feature of the grid of possible locations shown in Figure 7 is that we do not allow any inline offsets (skids). It is conceivable that in some circumstances a short distance skid may be more attractive than a crossline move — for example, when faced with a large linear obstacle perpendicular to the line that would otherwise require the point to be skipped. In our case, however, the obstacles were all approximately circular with diameters considerably larger than the station spacing. This considerably reduces the possibility of skidding points being successful; note,

Downloaded 11/14/22 to 76.133.148.255. Redistribution subject to SEG license or copyright; see Terms of Use at http://library.seg.org/page/policies/terms
DOI:10.1190/tle41110786.1

for example, in Figure 2c how little overlap the obstacle has with the line before the skid limit is reached. If skidding points is appropriate, then this is incorporated in the algorithm by simply decreasing the grid spacing in the inline direction. For the example presented here, we generated such a grid for a small section of the survey but found that the ability to skid points was not actually utilized due to the shape of the obstacles, so we only allowed crossline offsets for the full survey.

It is conceivable that obstacles centered on adjacent lines could result in the same points being selected by the algorithm for both lines. As each line is considered separately, this could be avoided by a number of different methods including offsetting the grids for adjacent lines in the inline and/or crossline direction or by forcing skids to points that have been selected on previous lines.

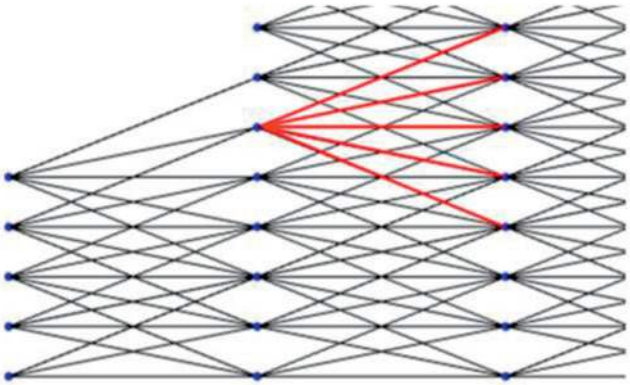

Figure 8. Diagram showing a series of possible paths between points. Note that the paths from one inline point to the next have a maximum angle of 22.5° to ensure that there are no sharp angles in the resulting lines.

Similar approaches could be applied if a minimum separation between sources and receivers is required.

Using these points, we create a series of paths that link the points. The angle of each path is limited (in this case) to 22.5° to ensure that they are smooth, preserving spatial continuity. Note that, depending on the spacing of the points, the limiting angle might not actually be achieved. For example, if we set the horizontal spacing to be 4 m and the vertical spacing 0.5 m, then the possible angles will be 0°, 14°, 26.5°, etc., and even though the theoretical angle limit might be 22.5°, the effective limit is only 14°. Once the optimum path between this network of points is identified, the resulting point positions are smoothed further in the crossline direction (in this case using a Savitzky-Golay filter).

By overlaying the paths onto the gridded vegetation map, such as that shown in Figure 6, we can calculate an environmental impact score for each path. We also wish to have the points as close to the original planned positions as possible, so we generate an offset score for each path based on the crossline distance of each path from the planned (straight) path. While in this case the distance between points does not vary significantly due to the 22.5° angle limit, we also assign a score based on the distance between points. (The closer the points are, the less time is spent traveling between them.) These scores are then weighted to give an overall weighting for each possible path. The histograms in Figure 9 show the resulting environmental, distance, and offset scores before and after application of the appropriate weightings — in this case we used values of 1, 1, and 10, respectively — and the final weightings for each path. Note that the overall weighted scores reflect the environmental scores most strongly, but the influence of the offset scores are also evident. This ensures that, if given a choice, the algorithm will default to paths that more closely follow the planned (straight) path.

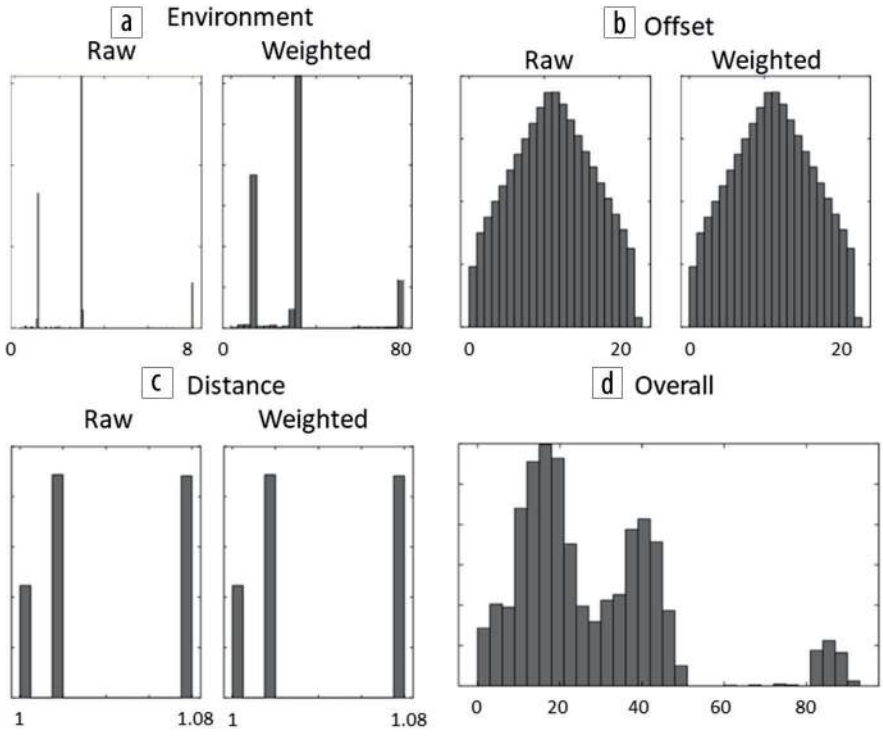

Figure 9. Histograms showing the raw and weighted (a) environmental, (b) offset, (c) distance, and (d) overall scores.

Those familiar with the field will recognize that what we have created is a directed graph (a *digraph* object in MATLAB), a series of nodes connected by directed edges. We can then use a shortest path algorithm (the *shortestpath* function in MATLAB) to find the lowest cost path along the line. Note that as the paths are weighted by their impact, the shortest path is not necessarily the straight line that connects the original planned points.

Figure 10a shows a section of the survey before the application of the impact-minimization process described here. Each point is color coded by its environmental impact (i.e., green points have no impact; red points impact vegetation greater than 2 m in height). Figure 10b shows the same section after the application of the algorithm. Note that the resulting paths all curve gently; i.e., spatial continuity is preserved. Overall,

Downloaded 11/14/22 to 76.133.148.255. Redistribution subject to SEG license or copyright; see Terms of Use at http://library.seg.org/page/policies/terms
DOI:10.1190/tle41110786.1

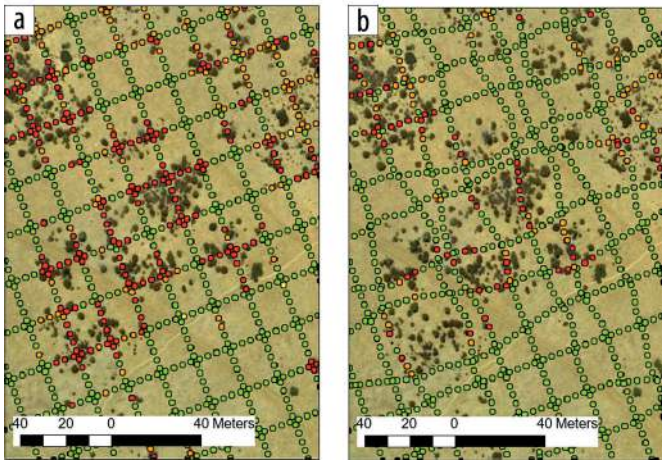

Figure 10. (a) Original survey points colored by their environmental impact and (b) after the application of the impact-minimization process described here. Overall, the impact on areas with vegetation greater than 2 m (red points) has been reduced by 68% and 0.3–2 m (orange points) by 34%.

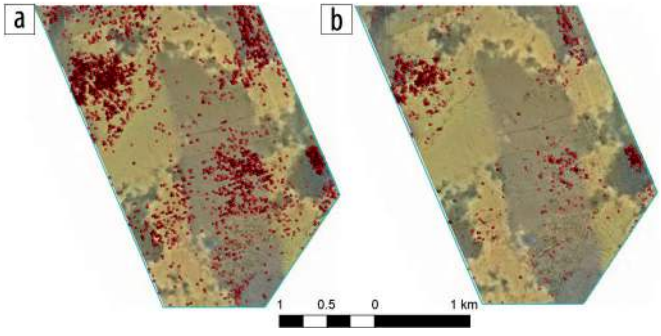

Figure 11. Scatter plot of a section of the survey showing areas with vegetation with a height greater than 2 m that would be cleared (a) before and (b) after application of the damage minimization process.

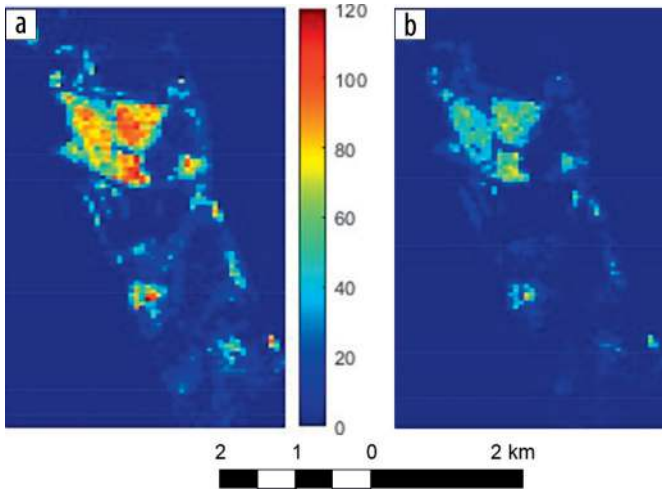

Figure 12. 2D histograms of the number of points impacting vegetation greater than 2 m in height (a) before and (b) after application of this process.

Figure 13. Image that shows a cultural heritage exclusion area (in red) through which the original, 24 m spaced, lines (in orange) clearly cut. The green circles show the lines after the application of the planning algorithm. They avoid both the exclusion area and the adjacent trees.

the impact on areas with vegetation height greater than 2 m has been reduced by 68% and on areas with vegetation height from 0.3 to 2 m by 34%. Due to our crossline move limitation, it was not possible to avoid all areas of vegetation. If this was a requirement, however, these points could be skipped.

Figure 11 is a scatter plot of a section of the survey that shows vegetation with a height greater than 2 m that would be cleared before (Figure 11a) and after (Figure 11b) the application of the vegetation impact-minimization process described here.

Figure 12 is a 2D histogram showing the number of survey points impacting vegetation greater than 2 m in height before (Figure 12a) and after (Figure 12b) the application of this process. Overall, the impact on greater than 2 m vegetation was reduced by 55%, on 0.3–2 m vegetation by 56%, and on 0–0.3 m vegetation by 61%. It should be noted that in this case the geometry was particularly dense, reducing our ability to offset the lines significantly. For less dense surveys, where these restrictions would not occur, the reduction is likely to be larger.

Discussion

The survey design process presented here is straightforward and can be applied automatically using standard mathematical software (in this case, MATLAB). Although the example shown primarily involves environmental obstacles that do not necessarily need to be avoided, it can also be applied to unavoidable obstacles such as cultural heritage sites (Figure 13) by giving prohibitively high weightings to paths that go through such areas.

Although similar to the approach described by Stork (2019), our process is based around paths and preserving spatial continuity, whereas Stork's approach involves creating a large number of possible points and then removing/moving points based on their cost and contribution to each bin. Although not currently implemented, additional weighted costs could be assigned to each path in a similar way for variables such as coverage contribution, accessibility, etc.

The reader is cautioned that the success of the algorithm, both in terms of preserving spatial continuity and generating logistically optimum line paths, is reliant on the appropriate selection of the grid point spacing (both inline and crossline if skips are to be considered) and the maximum allowable angle between consecutive points. For example, if the crossline grid spacing is too large, then the resulting detours may be unnecessarily large in both the crossline and inline dimensions.

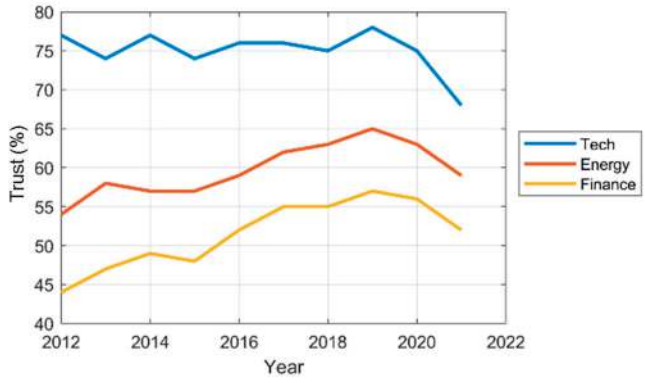

Figure 14. Trust survey results for selected industry sectors 2012–2021 (Edelman, 2021).

As awareness of the environmental effects of seismic surveys has increased (particularly offshore surveys, though increasingly so for onshore surveys as well), along with a general lack of trust (Figure 14) and in some cases opposition to the traditional (i.e., oil and gas) energy industry itself, the social license for acquiring seismic surveys has become increasingly threatened. Thus, the need to show that the environmental impacts of a survey have been minimized, through methods such as that presented here, is becoming increasingly important.

Conclusion

The automatic optimized survey design process described here shows how the environmental impact of seismic surveys can be reduced significantly. It enables the geophysicist to force the survey lines around rigid exclusion zones while simultaneously identifying paths that result in the least impact in areas where the objective is harm minimization. In our experience, the minimization of skipped points and the preservation of spatial continuity for deviated points, combined with modern processing techniques such as 5D interpolation (e.g., Trad, 2009), result in no noticeable degradation in quality of the resulting image. The approach does not currently introduce infill points, but it is conceivable that these could be added where total exclusion zones are problematic.

We hope that simple survey design methods such as those described here, along with improving acquisition technologies such as lightweight nodes (e.g., Dean et al., 2018), will reduce the environmental impact of our surveys (an objective we can all agree with) and improve our ability to operate in an increasingly restrictive environment. TLE

Acknowledgments

We would like to thank Neil Godber, Matt Grant, Jonathan Lowe, Michael Vincent, and Wilco Volwerk for their support of this project, along with excellent reviews by Dave Monk and Chengbo Li.

Data and materials availability

Data associated with this research are confidential and cannot be released.

Corresponding author: tim.dean.geo@gmail.com

References

Bastidas, C. H., and Y. Liu, 2019, Relocating source points outside exclusion zones on 3-D seismic survey designs: An optimized strategy: 89th Annual International Meeting, SEG, Expanded Abstracts, 298–302, https://doi.org/10.1190/segam2019-3215587.1.

Cordsen, A., M. Galbraith, and J. Peirce, 2000, Planning land 3-D seismic surveys: SEG, https://doi.org/10.1190/1.9781560801801.

Dabros, A., M. Pyper, and G. Castilla, 2018, Seismic lines in the boreal and arctic ecosystems of North America: Environmental impacts, challenges, and opportunities: Environmental Reviews, **26**, no. 2, 214–229, https://doi.org/10.1139/er-2017-0080.

Dawson, S. J., P. J. Adams, K. E. Moseby, K. I. Waddington, H. T. Kobryn, P. W. Bateman, and P. A. Fleming, 2018, Peak hour in the bush: Linear anthropogenic clearings funnel predator and prey species: Austral Ecology, **43**, no. 2, 159–171, https://doi.org/10.1111/aec.12553.

Dean, T., J. Tulett, and R. Barnwell, 2018, Nodal land seismic acquisition: The next generation: First Break, **36**, no. 1, 47–52, https://doi.org/10.3997/1365-2397.n0061.

Donze, T. W., and J. Crews, 2000, Moving shots on a 3-D seismic survey: The good, the bad, and the ugly (or how to shoot seismic without shooting yourself in the foot!): The Leading Edge, **19**, no. 5, 480–483, https://doi.org/10.1190/1.1438632.

Edelman, 2021, Edelman Trust Barometer, https://www.edelman.com/trust/2021-trust-barometer, accessed 13 October 2022.

Embar, K., B. P. Kotler, and S. Mukherjee, 2011, Risk management in optimal foragers: The effect of sightlines and predator type on patch use, time allocation, and vigilance in gerbils: Oikos, **120**, no. 11, 1657–1666, https://doi.org/10.1111/j.1600-0706.2011.19278.x.

Latham, A. D. M., M. C. Latham, M. S. Boyce, and S. Boutin, 2011, Movement responses by wolves to industrial linear features and their effect on woodland caribou in northeastern Alberta: Ecological Applications, **21**, no. 8, 2854–2865, https://doi.org/10.1890/11-0666.1.

Stork, C., 2019, Global land seismic acquisition optimization by accounting for varying noise, obstacles, non-uniform placement costs, and signal: 89th Annual International Meeting, SEG, Expanded Abstracts, 152–156, https://doi.org/10.1190/segam2019-3216861.1.

Trad, D., 2009, Five-dimensional interpolation: Recovering from acquisition constraints: Geophysics, **74**, no. 6, V123–V132, https://doi.org/10.1190/1.3245216.

Vermeer, G. J. O., 2012, 3D seismic survey design, Second edition: SEG, https://doi.org/10.1190/1.9781560803041.

Downloaded 11/14/22 to 76.133.148.255. Redistribution subject to SEG license or copyright; see Terms of Use at http://library.seg.org/page/policies/terms
DOI:10.1190/tle41110786.1